Posted on 16 Dec 2022 — The copyright holder is the author/funder. All rights reserved. No reuse without permission. — https://doi.org/10.22541/au.167120661.17798120/v1 — This a preprint and has not been peer reviewed. Data may be preliminary.

EPS8L1 promotes migration and metastasis of ovarian cancer by activating Rac1/MAPK signaling pathway via upregulating TIAM2

Yuting Wang[1], Lei Zhang[1], Xianqiang Luo[1], Meichen Wang[1], Min Luo[1], Hongyu Zhou[1], Limei Zhang[1], Yan Song[1], Junfei Zhang[1], Zhuomin Tan[1], Yinnong Jia[1], and Chen Qing[1]

[1]Kunming Medical University

December 16, 2022

Abstract

Background: EPS8L1, an analog of epidermal growth factor receptor pathway substrate 8 (Eps8), was screened out in our previous work from clinical samples of patients with ovarian cancer. Our studies also indicated that EPS8L1 might involve in various biological activities. In this study, we further investigated the effect and mechanism of EPS8L1 on the migration and metastasis of ovarian cancer. Methods: SKOV-3 cells with EPS8L1 overexpression and knockdown were established to perform in vitro scratch healing, transwell assay and actin-staining studies. Ovarian cancer mice with lung metastasis was established. Bioinformatics assay, qRT-PCR and Western blot were conducted to identify correlated proteins. Also, the Rac1 activity and the expression of MAPK pathway-related proteins were evaluated. Result: The knockdown of EPS8L1 inhibited the cellular migration in vitro and reduced tumors colonization in vivo. Actin-staining and ELISA experiment suggested that EPS8L1 regulated actin formation and cytoskeleton remodeling. Besides, mRNA and protein expression confirmed that EPS8L1 regulated the downstream molecule T-cell lymphoma invasion and metastasis 2 (TIAM2) and stimulated the activation of Rac1. Also, the phosphorylation levels of P38, Erk and Jnk in MAPK pathway decreased after EPS8L1 knockdown. Conclusion: The upregulation of EPS8L1 could promote migration and metastasis of ovarian cancer cells by regulating cytoskeleton remodeling. The mechanism underlying might be EPS8L1 regulates TIAM2 to induce Rac-GDP to Rac-GTP and then activates the downstream MAPK pathway. As a regulatory gene in cell migration and metastasis, EPS8L1 probably provide a new therapeutic target for ovarian cancer treatment.

Introduction

As one of the three major malignant tumors occurred in the female reproductive system, the incidence rate of ovarian cancer ranks third among gynecological malignant tumors, however, its mortality rate ranks top as high as 66% [1-2]. In clinic, 85%-90% of ovarian cancer is classified as epithelial ovarian cancer. Among them, serous cystadenocarcinoma are the most common pathological types, accounting for 40% in primary ovarian malignant tumors[3]. Recently, enhanced outcomes were observed for patients at the early stage of treatment with the improvement of clinical efficacy. However, most patients would experience relapse and eventually die as a result of systemic metastasis featured with ovarian cancer, resulting in the less than 30% of 5-year survival rate[4]. Therefore, the key for bringing a promising therapeutic strategy is the investigation on an effective target inhibiting the metastasis of ovarian tumors to significantly reduce the mortality rate.

In 1993, Fazioli *et al.* identified epidermal growth factor receptor kinase substrate 8 (Eps8) at the first time in fibroblasts[5]. Eps8 was consisted of an N-terminal phosphotyrosine binding (PTB) region, an intermediate Src-homology 3 (SH3) domain and a C-terminal effector region capping on the barbed end of filamentous actin to promote the elongation[6]. Three gene analogs are present for Eps8, namely epidermal growth factor receptor kinase substrate 8-like protein 1, 2 and 3 (EPS8L1, EPS8L2, and EPS8L3) [7].

Previous publications reported that overexpression of Eps8 promotes the proliferation of esophageal cancer

Posted on 16 Dec 2022 — The copyright holder is the author/funder. All rights reserved. No reuse without permission. — https://doi.org/10.22541/au.167120661.17798120/v1 — This a preprint and has not been peer reviewed. Data may be preliminary.

[8], non-small cell lung cancer [9] and pancreatic cancer[10], as well as migration and metastasis of oral squamous cell carcinoma [11], colon cancer[12] and breast cancer [13]. Later, Offenhauser *et al.* demonstrated Eps8 protein participated in cell migration and metastasis via activating the Rac-GEF of Sos-1 and inducing tyrosine kinase receptor-mediated cell remodeling by binding to actin [14].

In our previous work [15], tumor tissues from 31 patients with epithelial ovarian cancer and 10 adjacent normal tissue samples were collected in clinic and analyzed by the next generation sequencing (Fig.S1). As a result, EPS8L1 gene was screened out as a differentially expressed gene with high possibility to participate in the occurrence and development of epithelial ovarian cancer. Consistently, the bioinformatics analysis pointed out the clustered genes involved in the cell movement and migration. Therefore, EPS8L1 might regulate invasion and migration of tumor cells. However, the mechanism of EPS8L1 overexpression in ovarian cancer, especially in metastasis was not clearly elucidated.

To illustrate the role of EPS8L1 in the regulatory pathway, we analyzed the clinical information with the outcomes of patients with ovarian cancer. Additionally, *in vitro* and *in vivo* experiments were conducted to investigate the regulation of EPS8L1 on cell migration and metastasis. We found the downstream regulatory target-TIAM2, and explored the possible molecular mechanism of EPS8L1-induced migration and metastasis of ovarian cancer cells and the related pathways of Rac1-MAPK.

Methods

Cell culture and transfection

Human ovarian cancer cell lines SKOV-3 and ES-2 cells were purchased from the cell bank of Shanghai Institutes for Biological Sciences of Chinese Academy of Sciences. Cells were cultured in McCoy's 5A medium containing 10% fetal bovine serum (FBS), 100 IU/ml penicillin and 100 IU/ml streptomycin, at 37°C in a humidified environment with 5% CO_2.

For the lentiviral transfection, the Sh-RNA with the designed sequence (shown in Table S2 and S3) were applied. The design and package of the above lentiviruses were completed by Jikai Gene Company (Shanghai, China). The transfection MOI was determined according to the manufacturer's instructions, and the transfection time was 12 hours. When the transfected cells became stable, 1 μg/mL puromycin was added for 2-week incubation.

For the transfection of siRNA, cells were seeded in 6-well plates at the density of 10^5 cells per well, and transfected with relevant siRNA (80 pmol), followed by transfection with the LIPO3000 (Sigma) transfection reagent according to the manufacturer's instructions. Then, the expression ability of siRNA molecules was analyzed.

Scratch healing assay

After cells were seeded into 12-well plates at $3 \times 10^6$with 90%-100% confluency, the complete medium was discarded and treated with 4 μg/mL mitomycin C (GLPbio) for 1 h. A sterilized micropipette tip was applied to scratch the cell layer and the floating cells were washed off. Multiple spots on the scratch were imaged using a Zeiss microscope. Images were taken at 100x magnification. Cell migration measurements were performed using ImageJ software and the mobility ratio was calculated by the migrated area divided by original area.

Transwell migration assay

On a transwell migration plate (Corning, 8.0 μm pore size), 3×10^4 transfected SKOV-3 cells were resuspended in the upper chamber with 400 μL of serum-free McCoy's 5A medium and the lower chamber was filled with 500 μL McCoy's 5A medium containing 40 ng/mL EGF. After 24 h of incubation, cells invaded on the surface of the cavity were stained with 0.5% crystal violet and were imaged under fluorescence microscope. The number of migrated cells was counted using ImageJ software.

In vivo metastasis assay

Posted on 16 Dec 2022 — The copyright holder is the author/funder. All rights reserved. No reuse without permission. — https://doi.org/10.22541/au.167120661.17798120/v1 — This a preprint and has not been peer reviewed. Data may be preliminary.

The 2 to 3-week immunodeficient female Balb/c-nu mice (ASM Pharmaceutical Research Institute Co., Ltd., Hunan) were injected with 5×10^6 GFP-labelled SKOV-3 cells via the tail vein injection. After 8 weeks, the distribution of fluorescent signal was observed under a small animal *in vivo* imager (Bruker *in vivo* FX, Germany). After the whole-body imaging, the mice were sacrificed and dissected with organs imaged. For evaluation of pulmonary metastasis, lungs were cut into 5 μm and stained with H&E. Three sections throughout the whole lung per mice were screened, and the number of metastases was counted. In addition, the lungs were stained with MMP-2 and MMP-9 to quantify the expression levels of the corresponding proteins.

Immunohistochemistry (IHC) assay

After embedding with paraffin, the tumor tissues were remained in citrate antigen retrieval buffer (PH=6.0). Next, after blocking with 3% H_2O_2, the tissue was covered with 3% BSA at room temperature for 30 min. Then, primary antibody BMP6 (1:100, Abcam, ab155963), P-gp (1:1200, Abcam, ab170904) and p-ERK (1:200, Cell Signaling Technology, #5726) were added and incubated overnight at 4°C. After washing tissues with PBS, the corresponding secondary antibodies (HRP-labelled) were added and incubated at room temperature for 50 min. Then, freshly prepared diaminobenzidine (DAB) was added for color development, and then terminated by washing with water when the positive result displayed as brownish yellow color. Finally, tissues were counterstained with hematoxylin, dehydrated with alcohol, and mounted for microscopic examination. Three tumor tissues were randomly selected from each group to generate a total of 6 slices, and 3 high-magnification fields of each slice were randomly selected for scanning, and the positive area ratio was analyzed by ImageJ software. All the above reagents except antibodies were purchased from Wuhan Servicebio Technology CO., LTD (China).

Actin staining

The SKOV-3 cells were seeded in 24-well plates with 2×10^4 cells, cultured overnight, washed with PBS, placed on ice, fixed with 3.75% paraformaldehyde for 15 min, permeabilized with 0.5% Triton for 10 min, and finally stained with an appropriate amount of FITC-labelled phalloidin stock solution (Solarbio, #CA1640) for 15 min. After dripping DAPI on the slide, it was observed and recorded under a fluorescence microscope (Leica).

F-Actin quantification

F-Actin was quantified using an enzyme-linked immunosorbent assay kit (CUSABIO Human F-Actin ELISA Kit). The SKOV-3 cells were seeded with 2×10^5 in a 6-well plate. After washing with PBS, cells were scraped off and transferred to a 1.5mL centrifuge tube. Then a homogenous solution was generated by ultrasonic cell disruptor and stored overnight at -80°C. After thawing, the sample was centrifuged at 5000 × g, at 4 °C for 5min and supernatant was added to the embedded 96-well plate. The OD value of each well was measured based on the plotted standard curve under the wavelength of 450 nm to calculate the actual F-actin concentration.

Downstream genes screening

To explore the relevant targets for the mechanism of EPS8L1 in epithelial ovarian cancer, comprehensive database GENE EXPRESSION OMNIBUS (http://www.ncbi.nlm.nih.gov/geo) and public database String (https://cn.string-db.org/cgi/) were selected. To further confirm the relevant genes, RT-PCR assays with specific primers were performed. The mRNA expression levels of each gene in Sh-EPS8L1, OE-EPS8L1 and their corresponding vector control groups were obtained. After comparison of two groups, genes displaying large variance between cells were selected for the following verification and further verified by western blot assay.

Quantitative RT-PCR assay

Real-time quantitative PCR was performed using Trizol (Invitrogen) and reverse transcription using a high-capacity cDNA (Sigma) kit. TNNI3, TNNC1, TNNT2, CD44, TIAM2, TIAM1, MTA1, NM23, CD147, CD82,

EPS8L1 and GAPDH levels were measured using target primers (Invitrogen). Relative expression levels were measured by comparing the ratio of the Ct value of the target with the Ct value of GAPDH.

Rac1 activation assay

The PI3K-specific activator 740Y-P (20 μM) was added to cells in Sh-EPS8L1 and control groups for 24 h. Then, the SKOV-3 cells were scraped with cell lysate containing protease inhibitors. The lysates were centrifuged (10,000× g, 4 °C for 1 min) to remove cellular debris and then incubated with 10 μL of PAK-PBD beads from Rac1 Activation Kit (cytoskeleton, CAT#BK035-S) for 60 min at 4°C on a shaker. Beads were washed in 20 μL of 2 × Laemmli sample buffer and heated to boil for 2 min. Then, the determination of Rac1-GTP activation was performed with western blot experiments.

Western blot analysis

Cells were washed with phosphate buffered saline (PBS) and harvested with RIPA lysis collection buffer. Cell lysates were run on 10-15% SDS-polyacrylamide gels and then transferred to PVDF membranes, with primary antibodies incubated overnight at 4°C. After multiple washes, HRP-conjugated secondary antibody was added for 2 h at room temperature and developed with an ECL kit. Detection of active Rac1 protein requires pretreatment by pull-down assay. EPS8L1 antibody was purchased from Invitrogen (PA5-38746); TIAM2 antibody was purchased from Abcam (ab199426); Rac1 antibody was purchased from Abcam (ab155938); GAPDH antibody was purchased from in Affinity (AF7021).

Statistical analysis

The data were expressed as mean ± standard deviation (SD) and the results were analyzed with the statistical software SPSS 22.0. Each experiment was performed at least three times unless noted. If the data conformed to normal distribution and homogeneity of variance, two independent samples t-test was used for comparison between two groups, and one-way analysis of variance (ANOVA) was used for comparison between more than three groups. If the data did not conform to a normal distribution, a nonparametric rank sum test was used. The enumeration data were analyzed by the chi-square test. The value of $P< 0.05$ indicated that the difference was statistically significant. Figures were plotted by GraphPad Prism 7.

Results

EPS8L1 is overexpressed in epithelial ovarian cancer and correlated with poor clinical outcomes

In our previous work on the next generation sequencing of ovarian tumors from 31 patients, EPS8L1 was screened out with the possibility to participate in the tumor migration. To further validate the previous RNA-Seq results, we measured the expression of EPS8L1 gene in patients with serous ovarian cancer, which occurred with highest incidence among epithelial ovarian cancers. The preoperative venous blood from 43 patients with serous ovarian cancer were collected including the previously reported 31 patients, and the concentration of cfDNA from samples was detected by Qubit 2000. The results showed that no significant difference was observed in EPS8L1-cfDNA concentration from peripheral blood between patients with different ages, unilateral or bilateral tumors, classification, stages and with or without lymph node metastasis. To detect the relative level of EPS8L1-cfDNA in ovarian cancer patients, qPCR measurement was performed. Stage I and II were combined as early stage group, while stages III and IV were combined into advanced stage group. The difference in FIGO stage was statistically significant ($P = 0.000$), and the level of EPS8L1-cfDNA in patients with lymph node metastasis was significantly higher than that in patients without metastasis ($P = 0.000$) (Table 1). In addition, the expression of EPS8L1 in tumor tissues of 43 patients was detected by qRT-PCR, and the relationship between its mRNA expression and the clinicopathological indicators of patients was analyzed. Similarly, the results showed that the expression of EPS8L1 was not related to the patient's age, primary site and other factors, however, it was positively related to FIGO stages ($P = 0.031$) and lymph node metastasis ($P = 0.020$) (Table 2). The relationship between the expression of EPS8L1-mRNA in tissues and the clinicopathological indicators of patients was consistent with the results of cfDNA concentration, both suggesting that EPS8L1 might be related to the progression and metastasis

Posted on 16 Dec 2022 — The copyright holder is the author/funder. All rights reserved. No reuse without permission. — https://doi.org/10.22541/au.167120661.17798120/v1 — This a preprint and has not been peer reviewed. Data may be preliminary.

Posted on 16 Dec 2022 — The copyright holder is the author/funder. All rights reserved. No reuse without permission. — https://doi.org/10.22541/au.167120661.17798120/v1 — This a preprint and has not been peer reviewed. Data may be preliminary.

of epithelial ovarian cancer, and probably served as a new biomarker to predict clinical outcomes of ovarian cancer patients.

EPS8L1 is positively related to the migration and metastasis of tumor cells

We performed GO clustering analysis on EPS8L1 to identify relevant genes by different functions, including biological processes, cellular components and molecular functions. The results showed that among biological processes, cell-substrate adhesion was the key function with most gene clustered. Regarding to the cellular components, the collagen-like extracellular matrix was mainly clustered. In function, most genes were concentrated in the active part of endopeptidase. These results suggested that EPS8L1 might affect tumor invasion and metastasis through cell-extracellular matrix adhesion and other associated biological function (Figure 1a). The KEGG pathway enrichment showed that EPS8L1 was mainly overexpressed in signaling pathways such as vascular smooth muscle contraction, actin cytoskeleton regulation, and axonal pathways that positively related to the migration and motility of cells (Figure 1b). Using the TCGA database, we further analyzed the relationship between clinicopathological indicators and EPS8L1-mRNA expression in 379 patients with epithelial ovarian cancer. Consistently, the high expression of EPS8L1 was significantly related to the FIGO stages of patients ($P = 0.042 < 0.05$), shown in Table S1. The above results further demonstrated that EPS8L1 was positively related to the cellular invasion and migration.

EPS8L1 is differentially expressed in ovarian cancer cells and normal ovarian epithelial cells

The expression of mRNA and protein expression of EPS8L1 was evaluated in human normal ovarian epithelial cell line (IOSE80) and human epithelial ovarian cancer cell lines (Caov-3, 3AO, OVCAR3, A2780, SKOV-3, HO8910). As demonstrated in Figure 2a, the amount of EPS8L1-mRNA and EPS8L1 protein in all six human epithelial ovarian cancer cells were significantly higher than that of normal ovarian epithelial cells. Among six ovarian cancer cell lines, SKOV-3 cells exhibited highest concentration of EPS8L1-mRNA and EPS8L1 protein. In addition, SKOV-3 cells are typically serous ovarian cancer cells, as the most common types in epithelial ovarian cancer accounting for 30%-40% of primary ovarian malignant tumors. Therefore, the SKOV-3 cell line was selected for the following experiments including the establishment of EPS8L1 knockdown (Sh-EPS8L1) and overexpression (OE-EPS8L1) cells by lentivirus transfection (Figure 2b).

The knockdown of EPS8L1 inhibits migration of ovarian cancer cells

To study the effect of EPS8L1 on cell migration, the migration of SKOV-3 cells was detected by scratch healing assay after EPS8L1 knockdown. The quantification was represented by migration ratio, in which smaller value referred to the slower migration rate. The results showed that the migration ratio of Sh-EPS8L1 group (16.7%) was significantly lower than that of the control group (35.5%), with $P < 0.05$. The migration speed of Sh-EPS8L1 group was significantly lower than that of normal EPS8L1 group, indicating the regulation of cell migration by EPS8L1 (Figure 2c).

The knockdown of EPS8L1 inhibits cellular actin formation and cytoskeleton remodeling

Multiple G-actin are linked together to form actin chains and two strings of actin chains are twisted into fibrillar actin (F-actin), which constitutes the cytoskeleton of eukaryotes, and is closely related to the chemotactic ability of cells [16]. To validate that EPS8L1 induce cell migration and metastasis through cytoskeleton remodeling, FITC-labeled phalloidin was used to stain with F-actin in Sh-EPS8L1 and EPS8L1 (as control) cells. As observed by a fluorescence microscope, cells in control group demonstrated higher concentration and brighter intensity of filopodia enabling cells migrate in one direction. In contrast, the amount of filopodia in Sh-EPS8L1 cells was significantly reduced and no filopodia with invasive structures were detected indicating the inhibition of filopodia formation by suppressing EPS8L1.

After 24 h starvation without serum, 40 ng/mL EGF was given to stimulate the cells in both groups for 3 min. As shown in Figure 2d, the polymerization of cortical actin was observed and the amount of central actin bundles decreased in control group. It indicated that EGF stimulation induced the reorganization of cortical actin which generated the remodeling of cytoskeleton and enhanced the migration ability of cells. In contrary, cells in the Sh-EPS8L1 group exhibited no obvious response to EGF stimulation.

Posted on 16 Dec 2022 — The copyright holder is the author/funder. All rights reserved. No reuse without permission. — https://doi.org/10.22541/au.167120661.17798120/v1 — This a preprint and has not been peer reviewed. Data may be preliminary.

The ELISA kit was used to quantify the amount of F-actin in two groups. The results showed that the amount of F-actin in cells with low EPS8L1 expression was 3.67 mg/mL, while that in the control cells with normal EPS8L1 expression was 6.39 mg/mL. The difference between two groups was statistically significant with P <0.05 (Figure 2e). These results suggested that EPS8L1 promote the migration and metastasis of ovarian cancer cells by regulating the formation of filopodia and cytoskeleton remodeling.

The knockdown of EPS8L1 inhibits metastasis and colonization of ovarian tumor cells *in vivo*

To further verify the effect of EPS8L1 on metastasis of ovarian cancer, the *in vivo* metastasis experiments were performed. Two groups of ovarian cancer cells labelled with GFP fluorescent tags, GFP-Sh-EPS8L1 and GFP-EPS8L1 (control), were injected into the immunodeficient mice through the tail vein to allow tumor growth. After 8 weeks, mice were anesthetized and imaged by Bruker *in vivo* Fx to evaluate the colonization and distribution of GFP-labelled ovarian cancer cells. As compared with the Sh-EPS8L1 group, obviously local fluorescence enhancement was observed in the lungs of mice in control group suggesting the development of lung metastasis. In contrast, the low expression of EPS8L1 in ovarian cancer decreased the metastasis and colonization. Furthermore, tumors in the control group were shown to be more widely distributed throughout the body than that of Sh-EPS8L1 group, especially in the lymph nodes located on both sides of the neck of mice (Figure 3a). Then mice were sacrificed and dissected to evaluate the tumor growth in lungs. As shown in Figure 3b, higher amount of tumor cells was observed at lungs in the control than that in the Sh-EPS8L1 groups. In Figure 3c, the H&E staining quantification demonstrated that mice injected with control cells with normal SKOV-3 expression displayed significantly higher intensity of tumors per lung slice compared to mice injected with Sh-EPS8L1 cells (median 22 ± 1.78 *vs.* 4.6 ±1.01). More photographs for mice and the ink staining experiment for the lungs with metastasis to demonstrate the location of small tumor lesions were shown in Fig. S2.

The matrix metalloproteinase (MMP) family regulated the extracellular matrix degradation and cell adhesion remodeling to promote tumor cells diffusion and angiogenesis, which played an important role in tumor invasion and metastasis [17]. To further explore the mechanism of lung metastasis induced with ovarian cancer cells, immunohistochemistry was carried out by staining lung tissue slice of animals for MMP-2 and MMP-9 proteins. It was demonstrated the ratios of MMP-2 and MMP-9 protein expression in the Sh-EPS8L1 group were 0.719±0.09 and 0.111±0.02, respectively. In contrast, the MMP-2 and MMP-9 protein in the control group were 0.992±0.00 and 0.990±0.00, respectively. As compared in Figure 3d, the difference between two groups was statistically significant with MMP-2 (P <0.05) and MMP-9 (P <0.01) indicating that EPS8L1 promote the metastasis of ovarian cancer cells *in vivo* by regulating the expression of MMP-2 and MMP-9.

EPS8L1 regulates the expression of downstream TIAM2

To evaluate the dataset of OMNIBUS, Spearman correlation analysis were generated (Figure 4a). Moreover, a public database String (https://cn.string-db.org/cgi/) and online analysis (http://gepia.cancer-pku.cn/) were recruited to analyze genes related to EPS8L1 (Figure 4b and Fig.S3). It was found genes TIAM2 (r=0.470,P <0.001), TNNT2, TNNC1, and TNNI3 (all r=0.67,P <0.05) possibly related to EPS8L1(Fig. S4).

The RT-PCR results showed at mRNA level that EPS8L1 was highly expressed in OE-EPS8L1 and low expressed in Sh-EPS8L1 which was consistent with our experimental design. In addition, the expression of TNNT2, CD82, TIAM1, and TIAM2 was significantly different between OE-EPS8L1 and Sh-EPS8L1, with 46.64-fold (P<0.01), 13.37-fold (P<0.01), 9.71-fold (P<0.01) and 4.61-fold (P<0.01), respectively (Figure 4c).

Subsequently, four groups of SKOV-3 cells with OE-EPS8L1 or Sh-EPS8L1 or their corresponding vectors as control groups were used to evaluate the related genes at protein level. The results showed that among the above-mentioned differential genes, only TIAM2 gene was obviously regulated by EPS8L1 at protein level (Figure 4d). The decreased EPS8L1 expression resulted in the decreased TIAM2 expression, while increased EPS8L1 expression also increased TIAM2 expression. The TNNT2 gene with the greatest difference at the mRNA level show no significant difference at the protein level, which might be a transcription factor and

Posted on 16 Dec 2022 — The copyright holder is the author/funder. All rights reserved. No reuse without permission. — https://doi.org/10.22541/au.167120661.17798120/v1 — This a preprint and has not been peer reviewed. Data may be preliminary.

plays a role in post-transcriptional regulation. Otherwise, it is a protein with short half-life and difficult to be captured. We also performed corresponding validation in EPS8L1-overexpressing ES-2 cells, and the results were similar to those in SKOV-3 cells (Fig. S5). Therefore, TIAM2 was positively related to EPS8L1 and directly regulated by EPS8L1.

To clarify the regulatory relationship between EPS8L1 and TIAM2, small interfering RNA (siRNA) was utilized to knock down EPS8L1 and TIAM2 in SKOV-3 cells, respectively. Three sequences in each gene was used to measure gene expression and validate the knockdown efficiency to select suitable sequences for subsequent experiments. As shown in Figure 4e, the protein expression of TIAM2 decreased when EPS8L1 was knocked down. Contrarily, no significant change of EPS8L1 expression was observed with TIAM2 knockdown. These results verified our speculation that EPS8L1 is an upstream regulatory molecule of TIAM2, and TIAM2 is a downstream molecule of EPS8L1 (Figure 4f).

EGF activates the conversion of Rac1-GDP to Rac1-GTP by stimulating EPS8L1

When Eps8 forms a complex with Abi1 and Sos1, it regulates the depolymerization and assembly of microtubules through actin, and activates signaling pathways including Rac1-GTPase, thereby regulating the cytoskeleton [18]. To investigate whether EPS8L1 promotes the activation of Rac1 in SKOV-3 cells, Rac1-GTP concentration was measured with EGF.

After stimulating Sh-EPS8L1 with EGF, the expression of EPS8L1 increased with the prolongation of stimulation time. Simultaneously, the expression of TIAM2 increased as well. As shown in Figure 5a, total Rac1 amount was unchanged and the amount of Rac1-GTP increased. However, in the TIAM2-knockdown SKOV-3 cells (TIAM2-Si), EGF stimulation did not induce any change in TIAM2 expression, neither Rac1 activation was responded (Figure 5b). At the same time, scratch healing (Figure 5c) and transwell migration (Figure 5d) experiments were performed to evaluate migratory ability of cells responded to EGF stimulation after EPS8L1 and TIAM2 knockdown. The results were consistent with protein expression experiments. After TIAM2 knockdown, migration of the cells to all directions were reduced. Without TIAM2, this pathway induced by EPS8L1 was impaired at some extent.

PI3K agonist induces TIAM2 expression

As reported, PI3K mediated the activation of Rac1 through TIAM2[19]. Accordingly, we speculated that EPS8L1 might mediate the activation of Rac1 through TIAM2. 740Y-P is a cell-permeable phosphopeptide that binds to the p85 subunit of PI3K with high affinity to activate PI3K [20]. As demonstrated in Figure 6a, the expression of TIAM2 was restored after 740Y-P treatment, while the levels of EPS8L1 and Rac1-GTP activation did not recover compared to the control group. Thus, PI3K agonist could stimulate TIAM2, however, the activation of Rac1 by TIAM2 was mostly regulated by the expression of EPS8L1 as a decisive role in the EPS8L1-TIAM2 driven Rac1 activation.

EGF activates the MAPK pathway by stimulating EPS8L1

Noticeably, MAPK signaling pathway participates in the degradation of extracellular matrix, adhesion, motility and angiogenesis in tumor cells[13]. Thus, we hypothesized MAPK pathway might be a downstream pathway regulated by EPS8L1 after activating Rac1. As shown in Figure 6b, the phosphorylation levels of P38, Erk, and Jnk in the MAPK pathway decreased significantly in the Sh-EPS8L1 group compared with the control group, without affecting the amount of total proteins. After stimulation with EGF, the phosphorylation levels of P38, Erk and Jnk in the Sh-EPS8L1 group were still lower than those in the control group indicating the suppression of EPS8L1 lead to the inactivation of MAPK pathway. These results suggested that the MAPK signaling pathway contributed in EPS8L1-mediated metastasis and migration of ovarian cancer cells.

Discussion

Most ovarian cancer patients are in advanced stage (stage III-IV) at the first time of diagnosis with the high mortality rate. Unfortunately, majority of patients with ovarian cancer developed metastases at the

Posted on 16 Dec 2022 — The copyright holder is the author/funder. All rights reserved. No reuse without permission. — https://doi.org/10.22541/au.167120661.17798120/v1 — This a preprint and has not been peer reviewed. Data may be preliminary.

peritoneum, liver, and lymph nodes. As no well-defined therapeutic target has been discovered for ovarian cancer, the lack of effective therapy leads to no remarkable improvement of 5-year survival rate.

As the main cause of death in ovarian cancer patients, metastasis is closely related to clinical efficacy and prognosis of patients. Studies have shown that Eps8 gene is related to the proliferation of tumor cells[21]. In addition, the higher expression of Eps8 in metastases, probably participates in the integrin-dependent Rac1 pathway [11], cytoskeleton alteration[23] and regulation of focal adhesion kinase[24]. Wang *et al.* suggested that the high expression of Eps8 promoted the invasion and metastasis of head and neck squamous cell carcinoma [25]. Moreover, knockdown of Eps8 expression greatly reduces the ability of glioblastoma to invade and metastasize [26]. As demonstrated, Eps8 formed a tri-complex Eps8-Abi1-Sos1 to participate in the signal transduction to regulate Rac activity in epithelial mesenchymal transition (EMT) of ovarian cancer cells [27,28], however, the complex was not detected in non-metastatic cells. Welsch *et al.* reported the higher expression of Eps8 in pancreatic cancer cells of different origins by qRT-PCR which lead to invasion [29].

Eps8 gene is believed to regulate the migration and metastasis of tumor cells, among which EPS8L1 as the most important homologous might induce the major function. However, no study has been reported on the mechanism of EPS8L1 in tumors. In our previous work, EPS8L1 was screened out as up-regulated expression in the clinical ovarian cancer samples[15]. To further illustrate the mechanism of EPS8L1 in ovarian cancer, especially in the tumor migration and metastasis, we conduct this study.

The analysis of 43 clinical cases collected demonstrated that EPS8L1 was related to FIGO staging and lymph node metastasis of ovarian cancer indicating that EPS8L1 might closely related to the metastasis of ovarian cancer. Also, the knockdown of EPS8L1 decreased the migration speed of ovarian cancer cells in the scratch healing and transwell experiments. To exclude the possibility that scratch closure caused by cell proliferation, cells were pretreated with a low concentration of mitomycin C, a non-specific cytotoxic drug for cell cycle. The concentration of mitomycin C was selected to inhibit cell proliferation but not cell migration [30] to guarantee the movement was only induced by migration.

Regarding to the establishment of *in vivo* model with metastasis and invasion of ovarian cancer cells, orthotopic transplantation[31], footpad injection[32], intraperitoneal injection[33] and tail vein injection[34] have been reported previously. Originally, SKOV-3 cells were injected to mice intraperitoneally in the early stage to simulate the progress of intraperitoneal dissemination and metastasis to adjacent organs that are consistent to ovarian cancer patients in clinic. However, 4-5 weeks after intraperitoneal injection, malignant ascites was formed in the abdominal cavity of the mice, and the overall condition of mice was poor. Although the colonization of tumors was observed in abdomen, metastasis in lung, liver and other organs were not detected. Then, vein injection was selected with the superior effect to establish metastatic model. To monitor and evaluate tumor growth and distribution, the injected SKOV-3 cells were labelled with GFP-fluorescence to provide images under Bruker *in vivo* Fx imager. In the EPS8L1 knockdown group, no fluorescence signal was detected in lung during whole body scanning, however, scattered distribution of tumor cells in lung could be observed in the direct scanning of dissected organs, which may be due to the difficult to penetrate the skin by low fluorescent intensity of few tumor cells.

In Pearson and Spearman analysis, a moderately strong correlation between EPS8L1 and TIAM2 ($r=0.48$, $p<0.001$) was found. TIAM2 is an analog of TIAM1, which is an important exchange factor that catalyzes the conversion of Rac1 from the inactive form of Rac1-GDP to the active form of Rac1-GTP, thus, called Guanine nucleotide Exchange Factor (GEF). Rac1 is an important member of the small G protein family, whose activation is very important during cell migration[35]. Besides, other members of the small G protein family, Rac, Cdc42 and Rho are involved in tumor cell motility. Rac proteins promote the formation of actin-rich membrane folds at the migration tip, called lamellipodia [36]. Cdc42 regulates cell polarity to manipulate the direction of cell movement[37]. Rho promotes the formation of compressive stress fibers and maintains the focal adhesions at the posterior of the cells [38].

Studies found that TIAM1-driven Rac1 activation is the key to the formation of lamellipodia and remodeling of cytoskeletal proteins[39-40] with extensive regulatory effects on cell migration and metastasis. In contrast

Posted on 16 Dec 2022 — The copyright holder is the author/funder. All rights reserved. No reuse without permission. — https://doi.org/10.22541/au.167120661.17798120/v1 — This a preprint and has not been peer reviewed. Data may be preliminary.

to the evidence that TIAM1 stimulated by Ras and Rac, the GEF activity of TIAM2 is more reliable on Rac than Ras [41]. Recently, TIAM2 overexpression was reported to be associated with tumor progression and unfavorable prognosis in pancreatic cancer [42]. Therefore, we investigated the relationship between EPS8L1 and TIAM2 as well as their effects on Rac1 activation under EGF stimulation.

Likely a downstream molecule regulated by EPS8L1, the expression of TIAM2 was positively related with EPS8L1. In addition, the expression of EPS8L1 and TIAM2 was increased simultaneously under EGF stimulation. Also, the increase of Rac1-GTP by the EGF stimulation to the Sh-EPS8L1 group displayed the recovery of Rac1 activation. As a substrate for EPS8L1, EGF stimulation increases the phosphorylation of EPS8L1 by epidermal growth factor receptor (EGFR), then enhances the function of downstream TIAM2 to activate Rac1. However, knockdown of TIAM2 in cells exhibited no response to EGF stimulation demonstrating the indicating the necessary participation of TIAM2 in EPS8L1-driven Rac1 activation. In consistent with the situation of lysophosphatidic acid or platelet growth factor stimulation, the activation of Rac1 was dependent on TIAM1[43]. Thus, as an analog of TIAM1, similar mechanism might work for TIAM2, as GEF in the activation of Rac1 by EPS8L1, especially induced by EGF.

Previous studies have found that growth factors bind to tyrosine kinase receptors to activate the PHn domain of PI3K and regulate TIAM1-driven Rac activation [44]. In addition, Eps8-Sos1 complex binds to the scaffold protein Abi1 through its SH3 domain and then binds to the P85 regulatory subunit of P13K to mediates Rac1 activation and actin remodeling [27-28]. In our study, the expression of TIAM2, restored by the PI3K agonist 740Y-P did not compensate for the reduced activation of Rac1 in EPS8L1 knockdown cells. Therefore, EPS8L1 was critically required and played a decisive role in the Rac activation pathway to activate Rac1 by TIAM2.

Previous studies have found that Rac1/Rac2 and Cdc42, from the small G protein family, are not limited to their effects on cell morphology, but also as effective activators in signaling cascades of Erk, Jnk, and P38 in MAPK pathway [45-46]. In ovarian cancer cells with EPS8L1 knockdown, the levels of p-P38, p-Erk, and p-Jnk were lower than those in the control group regardless of stimulating with EGF or not. suggesting that the MAPK signaling pathway as downstream regulated by EPS8L1.

Conclusion

In this study, the following conclusions could be made and depicted as Figure 7. EPS8L1 promotes the migration and metastasis of ovarian cancer cells, which was mainly stimulated by extracellular signals such as EGF. The overexpression of EPS8L1. activates the downstream TIAM2 to induce its GEF activity, which facilitates the conversion of Rac1-GDP to Rac1-GTP, and regulates downstream MAPK cascade signaling to affect cytoskeleton remodeling and ultimately promote the migration and metastasis of ovarian cancer cells. In addition, the mechanism of EPS8L1 in promoting metastasis may also be related to its regulation on the expression of MMP-2 and MMP-9. These results provide an important scientific basis for understanding the mechanism of EPS8L1 gene in the development of ovarian cancer, especially in the migration and metastasis. In future, EPS8L1 will be studied intensively as a novel biomarker for the diagnosis and effective targets for treatment and prognosis of ovarian cancer.

Acknowledgements

This work was supported by the National Natural Science Foundation of China (grants no. 81860463, no. 82160524 and no. 82160344), Yunnan Provincial Department of S&T-KMU Joint Foundation (no. 2018FE001-003 and no. 202101AY070001-068).

Disclosure of interests

All authors declare no conflict of interest.

Contribution to Authorship

Y.W. performed all the experiments and composed the manuscript. L.Z. provided human specimens, clinical information and data analysis. X.L., M.W., L.M.Z., Y.S., J. Z., Z.T., M.L., and H.Z. provided support with

Posted on 16 Dec 2022 — The copyright holder is the author/funder. All rights reserved. No reuse without permission. — https://doi.org/10.22541/au.167120661.17798120/v1 — This a preprint and has not been peer reviewed. Data may be preliminary.

data collection, experimental materials and techniques. Y.J. and C.Q. designed the research and revised the manuscript. All authors read and approved the final manuscript.

Ethics approval and consent to participate

This animal study was approved by the Institutional Animal Care and Use Committee (IACUC) of Kunming Medical University according to the laboratory guidelines for the ethical review of animal welfare (kmmu2020060). The Research Ethics Committee of the Yunnan Provincial Cancer Hospital approved the sample collection study. Written informed consent was provided by all patients before the treatment procedure was initiated.

Figure legends

Figure 1. EPS8L1 was closely related to the migratory and metastatic abilities of cells. (a) GO clustering analysis for EPS8L1. (b)Scattering plot of enriched KEGG pathways for EPS8L1.

Figure 2. Knockdown of EPS8L1 might impair cell migration by inhibiting cytoskeleton reorganization. (a) Western blot analysis of EPS8L1 protein expression in normal ovarian epithelial cells (IOSE80) and different ovarian cancer cells (CAOV3, 3AO, OVCAR3, A2780, SKOV-3, HO8910). qRT-PCR detection of EPS8L1-mRNA expression in normal ovarian epithelial cells and different ovarian cancer cells. Gray value analysis of EPS8L1 protein expression in normal ovarian epithelial cells and different ovarian cancer cells (compared with IOSE80 group: $*P$ <0.05, ** P <0.01, $***P$ <0.001) (b) Western blot analysis of EPS8L1 protein in wild-type strains (control), knockdown, overexpression groups and their respective empty vector groups in ovarian cancer cell lines. qRT-PCR was used to detect the expression of EPS8L1-mRNA in knockdown/overexpression stably transfected cell lines and the respective empty vector and wild-type strains; Gray value analysis of EPS8L1 protein knockdown/overexpression expression in stably transfected cell lines and the respective empty vector and wild-type lines (compared with Ctrl-Si group or Ctrl-OE group: $**P$ <0.01, $***P$ <0.001; compared with the NC group: no significance, $P > 0.05$) (c) The scratch assay image of control and Sh-EPS8L1 SKOV-3 cells at staring point and 24h using microscopy. Measurement were made using Image J. Scratch closure was expressed as a percentage of initial scratch area. Data are shown as mean ± SE, $*P$ <0.05. Data are representative of 3 independent experiments performed under identical experimental conditions. (d) Fluorescence micrograph of cells staining with phalloidin (for F-actin, green), DAPI (for nucleus, blue) and the merged images of control and Sh-EPS8L1 cells alone and with EGF (40ng/mL) treatment for 3 minutes. Images were acquired under identical parameters in 10μm scale bar. (e) Quantification of actin content in Sh-EPS8L1 and control groups by F-actin ELISA kit. Data are presented as mean±SEM; n[?]3. $***P$ <0.001.

Figure 3. Knockdown of EPS8L1 inhibits the ability of cells to metastasize and colonize in vivo. (a) Fluorescent images of control and Sh-EPS8L1 SKOV-3 cells carrying GFP fluorescence in nude mice taken by a Bruker *in vivo* FX imager to observe the fluorescence distribution. (b) The fluorescent intensity of lung tissue in mice xenografted with control and Sh-EPS8L1 cells carrying GFP fluorescence after dissection. (c) Tumors presented on the lung and the H&E staining of lung nodules (x100 &x400 magnification). Total number of the lung metastasis per section was determined. Data are shown as median +- SE; $**P < 0.01$ (n = 4-7 mice). In each mouse, 3 lung sections were examined using identical parameters. (d) Immunohistochemistry analysis of MMP-2 and MMP-9 in lung tissues (x200 &x400 magnification). The lung tissues of 3 mice were randomly selected in each group for analysis using Image J, and the proportion of positive cells was used as an indicator to compare with the control group. Data are shown as mean +- SE, $**P$ <0.01, $***P$ <0.001.

Figure 4. EPS8L1 regulated the expression of downstream molecule TIAM2. (a) Spearman analysis was performed on the dataset (GSE18520) in the GEO database. Correlation coefficient r=0.4-0.6 was considered as moderate correlation, $***P$ <0.001. (b) String network analysis related to EPS8L1 gene. TNNT2, TNNI3, TNNC1 were strongly associated with correlation coefficient r=0.71 (not shown). (c) The mRNA expression levels by qRT-PCR of each related gene in OE-EPS8L1, Sh-EPS8L1 and corresponding vector control cells, fold change = mRNA expression of OE-EPS8L1/ mRNA expression of Sh-EPS8L1.

Posted on 16 Dec 2022 — The copyright holder is the author/funder. All rights reserved. No reuse without permission. — https://doi.org/10.22541/au.167120661.17798120/v1 — This a preprint and has not been peer reviewed. Data may be preliminary.

Data were obtained by 3 independent experiments performed under identical experimental conditions and shown as mean +- SE, P <0.05 is statistically significant. (d) Western-blot analysis of protein expression in OE-EPS8L1 and Sh-EPS8L1 cells. Quantification of EPS8L1 and TIAM2 protein expressed as percentage of GAPDH. (e) The expression level of TIAM2 protein was detected, after knocking down EPS8L1 with siRNA. (f) The expression level of EPS8L1 protein was detected after knocking down TIAM2 with siRNA. Data were shown as mean +- SD (n=3), data of multiple groups were statistically analyzed by one-way ANOVA, *P <0.05, **P <0.01. ImageJ software analyzed the gray value of protein expression.

Figure 5. EGF activated the conversion of Rac1-GDP to Rac1-GTP by stimulating EPS8L1. (a-b) Activation of Rac1 in EPS8L1 and TIAM2 knockdown cells. Cells were lysed and equal amount of proteins were incubated with GST-PAK1 protein to extract GTP-Rac1. Expression of GTP-Rac1 was evaluated with western blot using an anti-Rac1 antibody. Data were shown as means +- SD (n=3), data of multiple groups were compared by one-way ANOVA, *P <0.05, **P <0.01. ImageJ software analyzed the gray value of protein expression. (c) Capacity for migration of EPS8L1-Si cells and TIAM2-Si cells and the consequence of EGF stimulate. Data were shown as mean +- SD (n=3), data of multiple groups were compared by Student's t test, *P <0.05, ***P <0.001. (d) Transwell assay showed the stimulating effects of EGF in EPS8L1-Si cells and TIAM2-Si cells. Data were shown as mean +- SD (n=3), data of multiple groups were compared by Student's t test, *P <0.05, **P <0.01.

Figure 6. EGF activated the MAPK pathway by stimulating EPS8L1. (a) Activation of Rac1 with PI3K agonist (740Y-P) for 24 hours in EPS8L1 knockdown cells. Cells were lysed and equal amount of proteins were incubated with GST-PAK1 protein to extract GTP-Rac1. Expression of GTP-Rac1 was evaluated with western blot using an anti-Rac1 antibody. (b) Activation of MAPK family with EGF (40ng/ml) stimulation in EPS8L1 knockdown cells. All data were shown as means +- SD (n=3), data of multiple groups were compared by one-way ANOVA, *P <0.05, **P <0.01, ***P <0.001. ImageJ software analyzed the gray value of protein expression Data were shown as mean +- SD (n=3).

Figure 7. Hypothetical scheme for the regulation of EPS8L1-TIAM2 on F-actin remodeling by EGF in ovarian cancer cells. The stimulation by EGF enhances the phosphorylation of EPS8L1, activates the downstream function of TIAM2, and induces its specific GEF activity, which in turn activates the conversion of Rac1-GDP to Rac1-GTP, regulates cytoskeleton remodeling and ultimately promotes the migration and metastasis of ovarian cancer cells.

Tables

Table 1. Relationship of plasma cfDNA concentration and EPS8L1-cfDNA level in 43 patients with ovarian serous cystadenocarcinoma.

Characteristic	Number of cases	Concentration of cf-DNA(ng/μL)	P	Relative level of EPS8L1-
Age				
<55	25	0.203±0.051	0.917	2.70±0.42
55	18	0.201±0.737		2.95±0.44
Primary tumor site				
unilateral	15	0.186±0.051	0.218	2.83±0.51
bilateral	28	0.210±0.064		2.79±0.41
Organization type				
High-grade serous ovarian cancer	30	0.201±0.064	0.954	2.78±0.45
Low-grade serous ovarian cancer	13	0.203±0.053		2.85±0.43
FIGO staging				
I+II	19	0.190±0.040	0.220	2.49±0.33
III+IV	24	0.211±0.072		3.05±0.35
Lymph node metastasis				
Yes	22	0.214±0.067	0.173	3.13±0.23

Posted on 16 Dec 2022 — The copyright holder is the author/funder. All rights reserved. No reuse without permission. — https://doi.org/10.22541/au.167120661.17798120/v1 — This a preprint and has not been peer reviewed. Data may be preliminary.

Characteristic	Number of cases	Concentration of cf-DNA(ng/μL)	*P*	Relative level of EPS8L1-
No	21	0.189±0.051		2.46±0.34

Table 2. The correlation between expression of EPS8L1-mRNA and clinicopathological indicators of patients

Characteristic	No. of cases	EPS8L1-mRNA	*P*
Age			
<55	25	2.579±0.506	0.987?¿?
55	18	2.576±0.735	
Primary tumor site			
unilateral	15	2.426±0.641	0.232
bilateral	28	2.659±0.579	
Organization type			
High-grade serous ovarian cancer	30	2.627±0.614	0.478
Low-grade serous ovarian cancer	13	2.487±0.154	
FIGO staging			
I+II	18	2.357±0.462	0.031
III+IV	25	2.737±0.652	
Lymph node metastasis			
Yes	20	2.352±0.490	0.020
No	23	2.775±0.634	

Reference:

[1] Sung H, Ferlay J, Siegel RL, Laversanne M, Soerjomataram I, Jemal A, et al. Global cancer statistics 2020: GLOBOCAN estimates of incidence and mortality worldwide for 36 cancers in 185 countries. CA Cancer J Clin. 2021; 0: 1–41. [2] Cao W, Chen HD, Yu YW, Li N, Chen WQ. Changing profiles of cancer burden worldwide and in China: a secondary analysis of the global cancer statistics 2020. Chin Med J (Engl). 2021; 134(7): 783-791. [3] Cho KR. Ovarian cancer update: lessons from morphology, molecules, and mice. Arch Pathol Lab Med. 2009 Nov; 133(11): 1775-81. [4] Penny SM. Ovarian Cancer: An Overview. Radiol Technol. 2020 Jul; 91(6): 561-575. [5] Fazioli F, Minichiello L, Matoska V, Castagnino P, Miki T, Wong WT, et al. Eps8, a substrate for the epidermal growth factor receptor kinase, enhances EGF-dependent mitogenic signals. The EMBO journal, 1993; 12(10): 3799-3808. [6] Tocchetti A, Confalonieri S, Scita G, Di Fiore PP, Betsholtz C. In silico analysis of the EPS8 gene family: genomic organization, expression profile, and protein structure. Genomics. 2003; Feb;81(2): 234-44. [7] Matoskova B, Wong WT, Salcini AE, Pelicci PG, Di Fiore PP. Constitutive phosphorylation of eps8 in tumor cell lines: relevance to malignant transformation. Mol Cell Biol. 1995 Jul; 15(7): 3805-12. [8] Bashir M, Kirmani D, Bhat HF, Baba RA, Hamza R, Naqash S, et al. P66shc and its downstream Eps8 and Rac1 proteins are upregulated in esophageal cancers. Cell Commun Signal. 2010 Jan 18; 8: 13. [9] Wen Q, Jiao X, Kuang F, Hou B, Zhu Y, Guo W, et al. FoxO3a inhibiting expression of EPS8 to prevent progression of NSCLC: A new negative loop of EGFR signaling. EBioMedicine. 2019 Mar; 40: 198-209. [10] Tod J, Hanley CJ, Morgan MR, Rucka M, Mellows T, Lopez MA, et al. Pro-migratory and TGF-β-activating functions of αvβ6 integrin in pancreatic cancer are differentially regulated via an Eps8-dependent GTPase switch. J Pathol. 2017 Sep; 243(1): 37-50. [11] Yap LF, Jenei V, Robinson CM, Moutasim K, Benn TM, Threadgold SP, et al. Upregulation of Eps8 in oral squamous cell carcinoma promotes cell migration and invasion through integrin-dependent Rac1 activation. Oncogene. 2009; 28: 2524-2534. [12] Maa MC, Lee JC, Chen YJ, Chen YJ, Lee YC, Wang ST, et al. Eps8 facilitates cellular growth and motility of colon cancer cells by increasing the expression and activity of focal adhesion kinase. J Biol Chem. 2007; 282: 19399-19409. [13] Chen C, Liang Z, Huang W, Li X, Zhou F, Hu X, et al. Eps8 regulates cellular proliferation and migration of breast cancer. Int J Oncol. 2015; 46: 205-214. [14]

Posted on 16 Dec 2022 — The copyright holder is the author/funder. All rights reserved. No reuse without permission. — https://doi.org/10.22541/au.167120661.17798120/v1 — This a preprint and has not been peer reviewed. Data may be preliminary.

Offenhäuser N, Borgonovo A, Disanza A, Romano P, PonzanelliI, et al. The eps8 family of proteins links growth factor stimulation to actin reorganization generating functional redundancy in the Ras/Rac pathway. Mol Biol Cell. 2004; 15: 91-98. [15] Zhang L, Luo M, Yang H, Zhu S, Cheng X, Qing C. Next-generation sequencing-based genomic profiling analysis reveals novel mutations for clinical diagnosis in Chinese primary epithelial ovarian cancer patients. J Ovarian Res. 2019 Feb 20; 12(1): 19. [16] Nurnberg A, Kitzing T, Grosse R. Nucleating actin for invasion. Nat Rev Cancer. 2011 Mar; 11(3): 177-87. [17] Kapoor C, Vaidya S, Wadhwan V, Hitesh, Kaur G, Pathak A. Seesaw of matrix metalloproteinases (MMPs). J Cancer Res Ther. 2016 Jan-Mar; 12(1): 28-35. [18] Scita G, Tenca P, Areces LB, Tocchetti A, Frittoli E, Giardina G, et al. An effector region in Eps8 is responsible for the activation of the Rac-specific GEF activity of Sos-1 and for the proper localization of the Rac-based actin-polymerizing machine. J Cell Biol. 2001 Sep 3; 154(5): 1031-44. [19] Cooke M, Kreider-Letterman G, Baker MJ, Zhang S, Sullivan NT, Eruslanov E, et al. FARP1, ARHGEF39, and TIAM2 are essential receptor tyrosine kinase effectors for Rac1-dependent cell motility in human lung adenocarcinoma. Cell Rep. 2021 Nov 2; 37(5): 109905. [20] Williams, EJ & Doherty, P. Evidence for and against a pivotal role of PI 3-kinase in a neuronal cell survival pathway. Mol. Cell. Neurosci. 1999; 13: 272–280. [21] Yang M, Huang CZ. Mitogen-activated protein kinase signaling pathway and invasion and metastasis of gastric cancer. World J Gastroenterol. 2015 Nov 7; 21(41): 11673-9. [22] Yap LF, Jenei V, Robinson CM, Moutasim K, Benn TM, Threadgold SP, et al. Upregulation of Eps8 in oral squamous cell carcinoma promotes cell migration and invasion through integrin-dependent Rac1 activation. Oncogene. 2009 Jul 9; 28(27): 2524-34. [23] Fregnan F, Petrov V, Garzotto D, De Marchis S, Offenhauser N, Grosso E, et al. Eps8 involvement in neuregulin1-ErbB4 mediated migration in the neuronal progenitor cell line ST14A. Exp Cell Res. 2011 Apr 1; 317(6):757-69. [24] Shahoumi LA, Khodadadi H, Bensreti H, Baban B, Yeudall WA. EPS8 phosphorylation by Src modulates its oncogenic functions. Br J Cancer. 2020 Sep; 123(7): 1078-1088. [25] Wang H, Patel V, Miyazaki H, Gutkind JS, Yeudall WA. Role for EPS8 in squamous carcinogenesis. Carcinogenesis. 2009 Jan; 30(1): 165-74. [26] Cattaneo MG, Cappellini E, Vicentini LM. Silencing of Eps8 blocks migration and invasion in human glioblastoma cell lines. Exp Cell Res. 2012 Sep 10; 318(15): 1901-12. [27] Scita G, Nordstrom J, Carbone R, Tenca P, Giardina G, Gutkind S, et al. EPS8 and E3B1 transduce signals from Ras to Rac. Nature. 1999 Sep 16; 401(6750): 290-3. [28] Innocenti M, Frittoli E, Ponzanelli I, Falck JR, Brachmann SM, Di Fiore PP, et al. Phosphoinositide 3-kinase activates Rac by entering in a complex with Eps8, Abi1, and Sos-1. J Cell Biol. 2003 Jan 6; 160(1): 17-23. [29] Welsch T, Endlich K, Giese T, Buchler MW, Schmidt J. Eps8 is increased in pancreatic cancer and required for dynamic actin-based cell protrusions and intercellular cytoskeletal organization. Cancer Lett. 2007 Oct 8; 255(2): 205-18. [30] Liang CC, Park AY, Guan JL. In vitro scratch assay: a convenient and inexpensive method for analysis of cell migration in vitro. Nat Protoc. 2007; 2(2): 329-33. [31] Yi XF, Yuan ST, Lu LJ, Ding J, Feng YJ. A clinically relevant orthotopic implantation nude mouse model of human epithelial ovarian cancer–based on consecutive observation. Int J Gynecol Cancer. 2005; 15(5): 850-5. [32] Fan L, Liu Y, Zhang X, Kang Y, Xu C. Establishment of Fischer 344 rat model of ovarian cancer with lymphatic metastasis. Arch Gynecol Obstet. 2014 Jan; 289(1): 149-54. [33] Rose GS, Tocco LM, Granger GA, DiSaia PJ, Hamilton TC, Santin AD, et al. Development and characterization of a clinically useful animal model of epithelial ovarian cancer in the Fischer 344 rat. Am J Obstet Gynecol. 1996 Sep; 175(3 Pt 1): 593-9. [34] Peng L, Ran YL, Hu H, Yu L, Liu Q, Zhou Z, et al. Secreted LOXL2 is a novel therapeutic target that promotes gastric cancer metastasis via the Src/FAK pathway. Carcinogenesis. 2009 Oct; 30(10): 1660-9. [35] Raftopoulou M, Hall A. Cell migration: Rho GTPases lead the way. Dev Biol. 2004 Jan 1; 265(1): 23-32. [36] Hall A. Rho GTPases and the actin cytoskeleton. Science. 1998; 279(5350): 509-14. [37] Nobes CD, Hall A. Rho, rac, and cdc42 GTPases regulate the assembly of multimolecular focal complexes associated with actin stress fibers, lamellipodia, and filopodia. Cell. 1995 Apr 7; 81(1):53-62. [38] Hall A, Nobes CD. Rho GTPases: molecular switches that control the organization and dynamics of the actin cytoskeleton. Philos Trans R Soc Lond B Biol Sci. 2000 Jul 29; 355(1399): 965-70. [39] Chiu CY, Leng S, Martin KA, Kim E, Gorman S, Duhl DM. Cloning and characterization of T-cell lymphoma invasion and metastasis 2 (TIAM2), a novel guanine nucleotide exchange factor related to TIAM1. Genomics. 1999 Oct 1; 61(1):66-73. [40] Mertens AE, Roovers RC, Collard JG. Regulation of Tiam1-Rac signalling. FEBS Lett. 2003 Jul 3;546(1):11-6. [41] Maltas J, Reed H, Porter A, Malliri A. Mechanisms and consequences of dysregulation of

Posted on 16 Dec 2022 — The copyright holder is the author/funder. All rights reserved. No reuse without permission. — https://doi.org/10.22541/au.167120661.17798120/v1 — This a preprint and has not been peer reviewed. Data may be preliminary.

the Tiam family of Rac activators in disease. Biochem Soc Trans. 2020 Dec 18; 48(6): 2703-2719. [42] Jiang B, Zhou L, Lu J, Wang Y, Liu C, Zhou W, et al. Elevated TIAM2 expression promotes tumor progression and is associated with unfavorable prognosis in pancreatic cancer. Scand J Gastroenterol. 2021 Jan; 56(1): 59-67. [43] Van Leeuwen FN, Olivo C, Grivell S, Giepmans BN, Collard JG, Moolenaar WH. Rac activation by lysophosphatidic acid LPA1 receptors through the guanine nucleotide exchange factor Tiam1. J Biol Chem. 2003 Jan 3; 278(1): 400-6. [44] Lambert JM, Lambert QT, Reuther GW, Malliri A, Siderovski DP, Sondek J, et al. Tiam1 mediates Ras activation of Rac by a PI(3)K-independent mechanism. Nat Cell Biol. 2002 Aug; 4(8): 621-5. [45] Bancroft CC, Chen Z, Dong G, Sunwoo JB, Yeh N, Park C, et al. Coexpression of proangiogenic factors IL-8 and VEGF by human head and neck squamous cell carcinoma involves coactivation by MEK-MAPK and IKK-NF-kappaB signal pathways. Clin Cancer Res. 2001 Feb; 7(2): 435-42. [46] Paine E, Palmantier R, Akiyama SK, Olden K, Roberts JD. Arachidonic acid activates mitogen-activated protein (MAP) kinase-activated protein kinase 2 and mediates adhesion of a human breast carcinoma cell line to collagen type IV through a p38 MAP kinase-dependent pathway. J Biol Chem. 2000 Apr 14; 275(15): 11284-90.

Hosted file

`Additional file 1.docx` available at https://authorea.com/users/566989/articles/613556-eps8l1-promotes-migration-and-metastasis-of-ovarian-cancer-by-activating-rac1-mapk-signaling-pathway-via-upregulating-tiam2

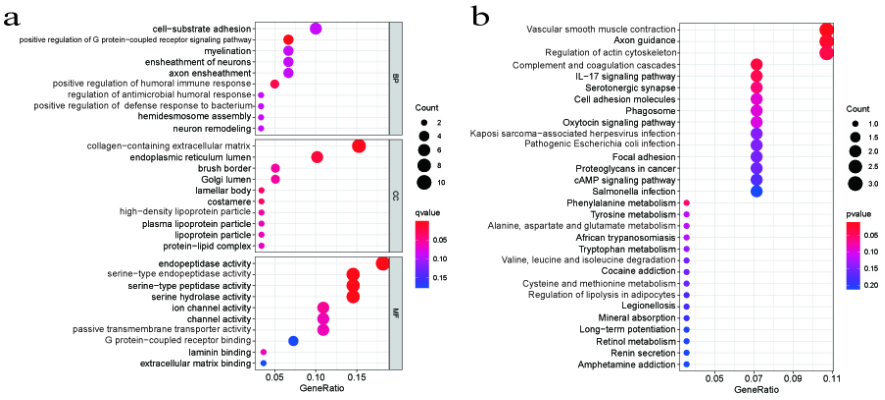

Posted on 16 Dec 2022 — The copyright holder is the author/funder. All rights reserved. No reuse without permission. — https://doi.org/10.22541/au.167120661.17798120/v1 — This a preprint and has not been peer reviewed. Data may be preliminary.

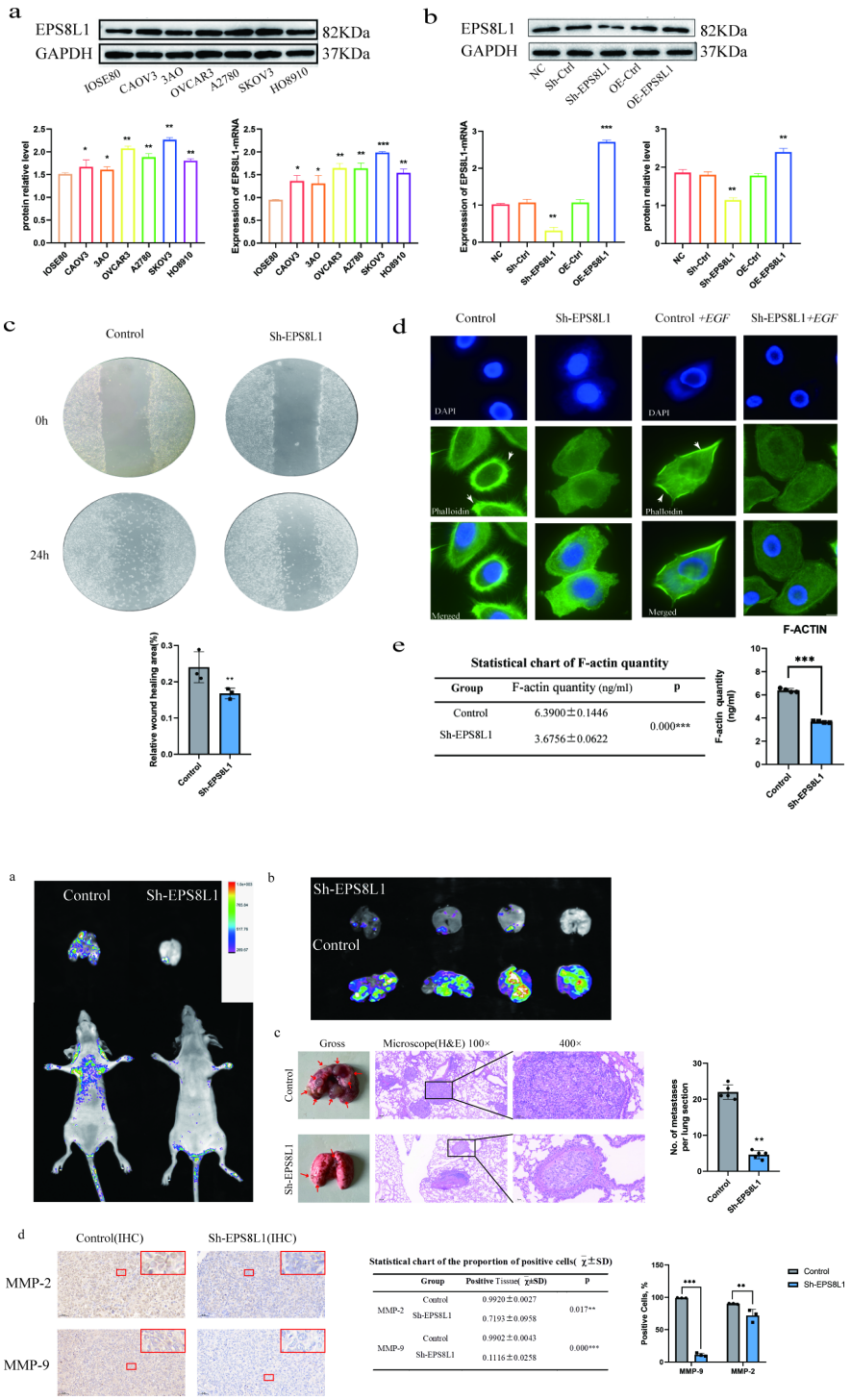

Posted on 16 Dec 2022 — The copyright holder is the author/funder. All rights reserved. No reuse without permission. — https://doi.org/10.22541/au.167120661.17798120/v1 — This a preprint and has not been peer reviewed. Data may be preliminary.

a

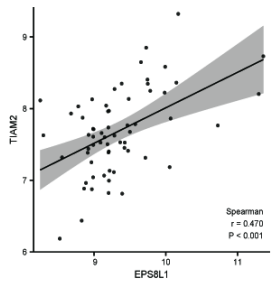

b

c

Gene name	OE-EPS8L1 group	Sh-EPS8L1 group	Fold change	*P*
EPS8L1	211.19±45.01	0.16±0.04	1087.72	0.000
TNNT2	25.17±10.92	0.54±0.12	46.64	0.004
CD82	6.71±2.47	0.5±0.23	13.37	0.000
TIAM1	4.87±2.02	0.5±0.12	9.71	0.000
TIAM2	5.35±0.98	1.16±0.38	4.61	0.000
MTA1	3.34±1.23	0.76±0.31	4.37	0.000
TNNC1	3.1±0.85	0.74±0.24	4.18	0.000
NM23	3.66±0.78	0.98±0.22	3.73	0.002
CD147	4.26±1.2	1.35±0.42	3.23	0.000
TNNI3	1.52±0.55	0.87±0.42	1.74	0.061
CD44	1.81±1.1	1.30±0.79	1.39	0.357

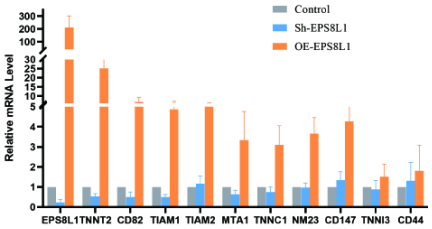

d

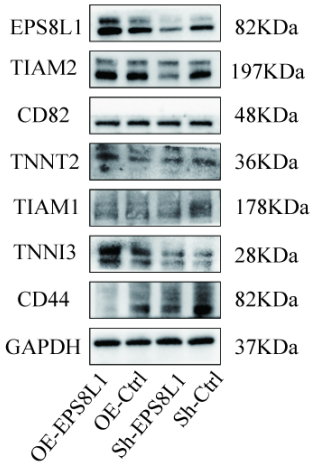

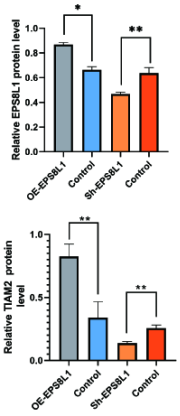

e

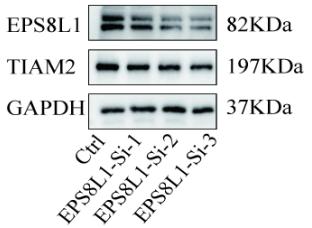

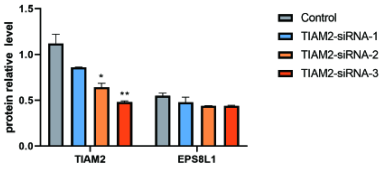

f

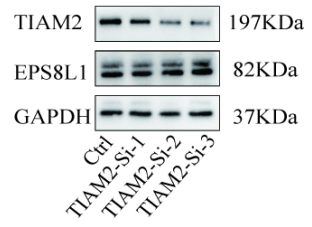

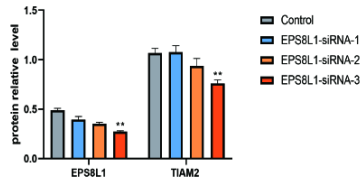

Posted on 16 Dec 2022 — The copyright holder is the author/funder. All rights reserved. No reuse without permission. — https://doi.org/10.22541/au.167120661.17798120/v1 — This a preprint and has not been peer reviewed. Data may be preliminary.

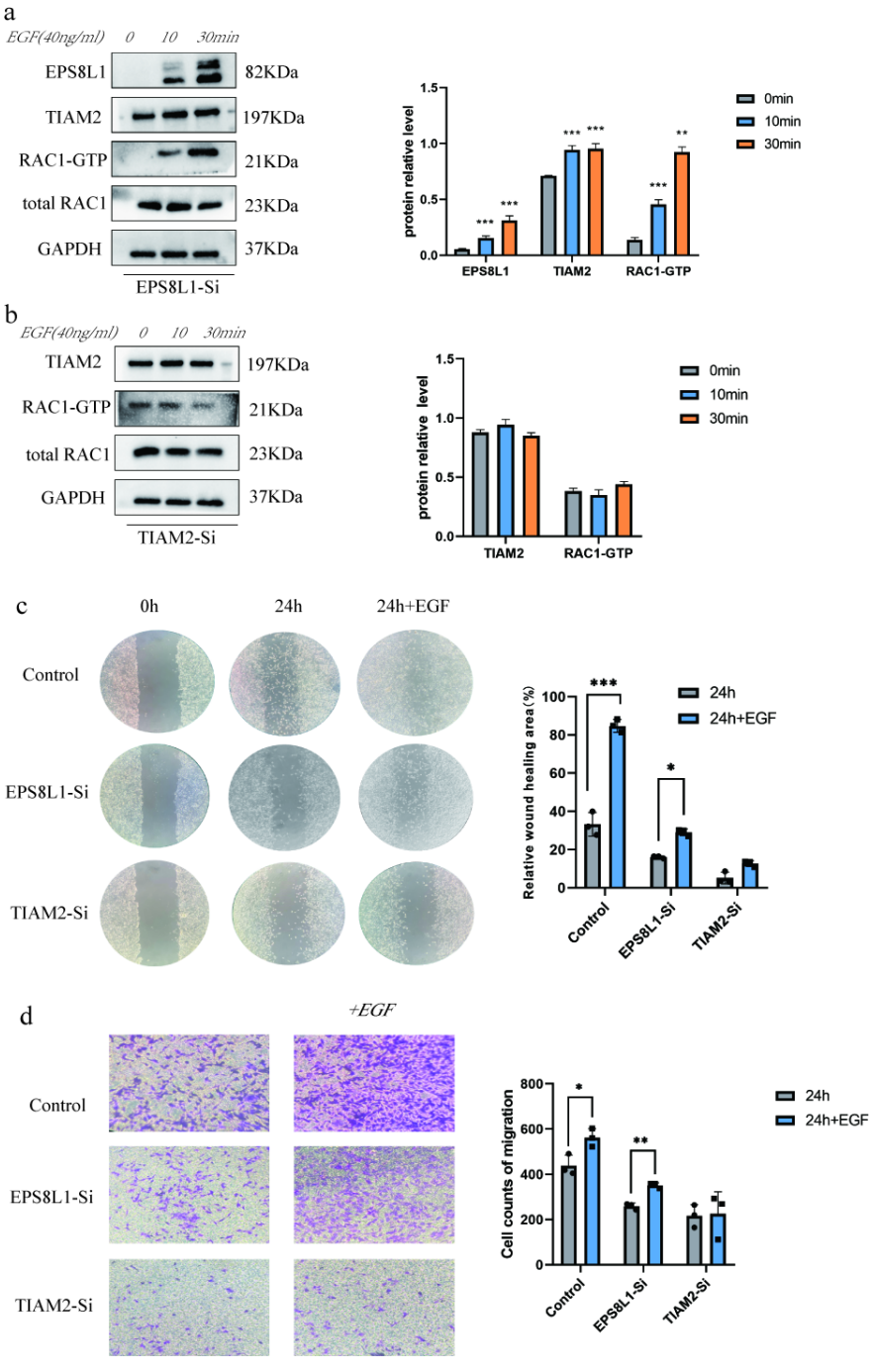

Posted on 16 Dec 2022 — The copyright holder is the author/funder. All rights reserved. No reuse without permission. — https://doi.org/10.22541/au.167120661.17798120/v1 — This a preprint and has not been peer reviewed. Data may be preliminary.